Bilateral Basal Ganglia Lesions: Pediatric Differential Considerations[1]

Vincent B. Ho, MD
Charles R. Fitz, MD
Sylvester H. Chuang, MD
Carl A. Geyer, MD

Computed tomography (CT) and magnetic resonance (MR) imaging have dramatically improved the ability to visualize the deep gray structures of the basal ganglia (primarily, the caudate nucleus, putamen, and globus pallidus). Any process that alters cerebral metabolism can lead to basal ganglia damage. This article presents the spectrum of disease that may be seen with bilateral basal ganglia abnormalities in the pediatric population. A simplified approach to the differential diagnosis of these entities is based on acute versus chronic conditions and radiologic manifestations. Acute processes include hypoxia, hypoglycemia, carbon monoxide poisoning, hemolytic-uremic syndrome, osmotic myelinolysis, and encephalitis. Chronic conditions include inherited ("inborn errors of metabolism," Huntington disease, and dysmyelinating diseases) or acquired (sequelae of acute disorders) conditions that represent abnormal biochemical or structural processes within the basal ganglia. Elimination of acute causes gives little hope for improvement. Recognition of chronic disorders is important for counseling purposes, since most of these conditions have specific patterns of inheritance.

1.   **2.**

Figures 1, 2.   Normal basal ganglia. **(1)** Axial T2-weighted magnetic resonance (MR) image of the brain of a healthy 3-year-old child shows the caudate nucleus (*C*), putamen (*P*), and globus pallidus (*G*). **(2)** Axial T2-weighted MR image of the brain of a healthy 8-year-old child shows the characteristic MR appearance of the basal ganglia. Abbreviations are the same as those in Figure 1. With normal maturation, there is progressive darkening of the T2-weighted signal intensity. This phenomenon, which occurs first in the globus pallidus (compare Figs 1 and 2) and later in the putamen, is thought to result from the progressive deposition of iron in these regions over time.

■ INTRODUCTION

The basal ganglia—comprised principally of the caudate nucleus, putamen, and globus pallidus (Figs 1, 2)—form the core of the extrapyramidal system. The basal ganglia receive projections from almost every region of the cerebral cortex, which enables them to integrate extrapyramidal motor activity. Historically, abnormalities in movement have been attributed to diseases of the basal ganglia; however, not all basal ganglia abnormalities manifest with a characteristic movement disorder. This apparent lack of neurologic specificity is particularly true of diffuse basal ganglia diseases encountered during childhood. With the clinical history and radiologic data, however, one may limit the differential considerations. In this article, we discuss this simplified approach to bilateral basal ganglia lesions. Additionally, the normal predisposing factors for basal ganglia injury are presented.

■ PREDISPOSING FACTORS

Buried within each cerebral hemisphere, the basal ganglia regulate extrapyramidal motor activity. This process is dynamic and demands chemical energy primarily in the form of aden-

osine triphosphate (ATP). The high energy requirement of the basal ganglia, in turn, mandates a rich blood supply and a high concentration of trace metals (1). Unfortunately, these same features make the basal ganglia vulnerable to systemic conditions both short and long term. This susceptibility for damage is especially true during childhood when the metabolic needs of the basal ganglia are greater (2).

● Metabolism

The metabolic requirements of the basal ganglia are attributable to their neurotransmissive role. The synaptic integration of information by the basal ganglia requires a ready supply of ATP. ATP is necessary to maintain the transmembrane ion gradients important for neuronal conduction and to regulate transmitter synthesis, release, and reuptake. Under normal conditions, ATP is efficiently produced by aerobic respiration and oxidative phosphorylation (Fig 3) within mitochondria (1–4).

The acute deprivation of oxygen (hypoxia, carbon monoxide poisoning) or glucose (hypoglycemia) results in insufficient and inefficient production of ATP via anaerobic routes and in diffuse basal ganglia damage (5–10).
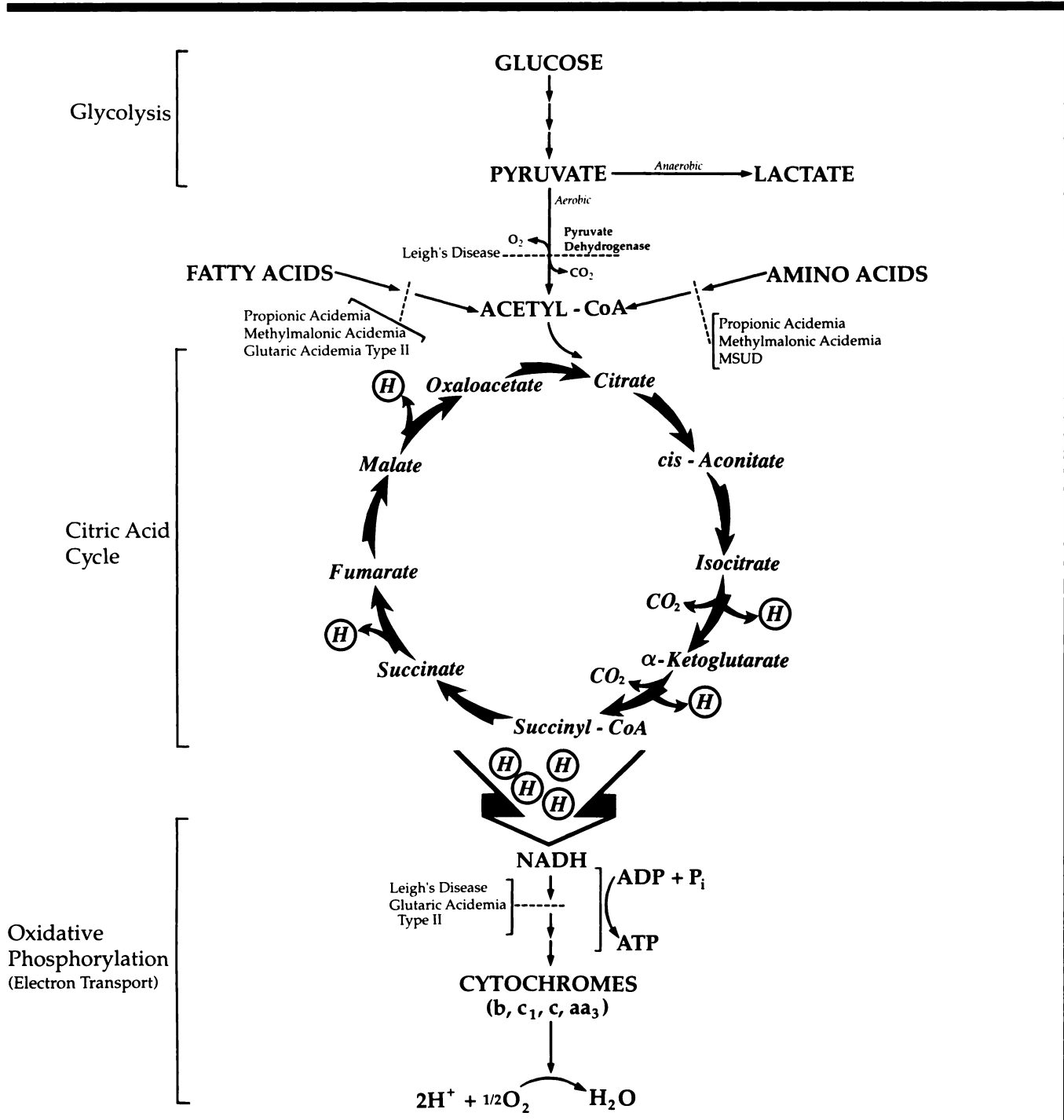
Figure 3. Basal ganglia metabolism. Drawing shows that the production of ATP by the mitochondria requires a variety of biochemical pathways (simplified here). Most entities that preferentially affect the basal ganglia do so by altering basal ganglia metabolism. Dashed lines = the proposed sites of metabolic abnormality (also simplified) seen with these disorders, ADP = adenosine diphosphate, CO_2 = carbon dioxide, H = hydrogen, H_2O = water, $MSUD$ = maple syrup urine disease, $NADH$ = reduced nicotinamide adenine dinucleotide, O_2 = oxygen, P_i = inorganic phosphate. (Courtesy of Venetia E. Valiga, Department of Scientific Illustrations, Armed Forces Institute of Pathology, Washington, DC.)

Similarly, long-term abnormalities in aerobic respiration (Leigh disease, "lactic acidemias," glutaric acidemia type II) or mitochondrial structure (mitochondrial cytopathy) lead to basal ganglia injury (4,11). Disorders that limit the processing of other energy substrates, such as amino acids and fatty acids, for use in the citric acid cycle (maple syrup urine disease, glutaric acidemia type II, propionic aciduria, methylmalonic aciduria) also result in basal ganglia damage (1,4,11).

The high metabolic rate of the basal ganglia rivals that of the cerebral and cerebellar cortices (1,2). By using fluorodeoxyglucose positron emission tomography, Chugani et al (2) showed the basal ganglia metabolic rate of children to be especially increased, greater than that of the adult. The additional energy demand of the basal ganglia during childhood can be attributed to that of normal development, which includes that required for myelination (10).

Figure 4. Normal brain perfusion. Axial tomogram from a technetium hexamethyl-propylene-amine oxime study of a healthy young child demonstrates the marked increased vascularity of the basal ganglia, which is comparable to that of the cerebellum.

● **Vascularity**

The metabolic needs of the basal ganglia are matched by their marked vascularity (Fig 4) (1). A rich vascular bed is necessary to provide nutrients and substrates for the active metabolism of the basal ganglia and to remove unwanted metabolic by-products. Interruption of the vascular supply of the basal ganglia (strangulation, as in child abuse, or microthrombosis, as in hemolytic-uremic syndrome) results in their injury (4–9). Additionally, the vascular nature of the basal ganglia may predispose the child to an infection carried in the blood (such as encephalitis).

● **Trace Metals**

The basal ganglia house high concentrations of trace metals such as iron, copper, and manganese (1,12,13). These trace metals, iron in particular, are important cofactors necessary for the normal metabolic activity of the basal ganglia. However, these same trace metals may also be involved in deleterious biochemical reactions (1,6,14). Iron, for example, catalyzes the production of destructive oxygen free radicals by means of the Haber-Weiss reaction. The normally higher concentration of trace metals within the basal ganglia may accentuate their vulnerability to altered metabo-
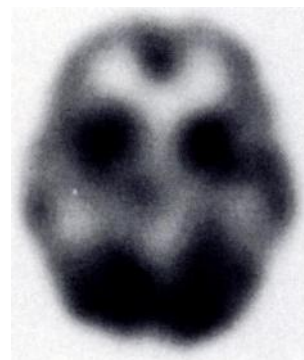
lism. Additionally, the toxic accumulation of trace metals such as iron (Hallervorden-Spatz disease), copper (Wilson disease), and manganese (chronic manganese intoxication) may result in destruction of the basal ganglia (1,15).

The high concentrations of iron in the basal ganglia are believed to account for their characteristic MR imaging signal intensities, a feature that increases the conspicuity of basal ganglia abnormalities. Iron, more specifically iron compounds such as ferritin, is paramagnetic and thus detectable on MR images (16–19). Iron creates local inhomogeneity within the magnetic field and dephases the spin, resulting in a signal dropout (T2* effect) that is best appreciated on T2-weighted MR images. The degree of signal loss on MR images varies with both the concentration of iron and the strength of the magnetic field of the imager. The MR imaging detection of iron has been theorized to begin at concentrations of 10–15 mg/100 g (19).

Initially, the signal intensity of the basal ganglia approximates that of the cerebral cortex. However, with the normal increase in basal ganglia iron, which occurs with aging, there is progressive darkening of the signal intensity of the basal ganglia on MR images. At age 6 months, the globus pallidus becomes increasingly dark on T2-weighted MR images (T2* effect), a process that progresses

Table 1
Childhood Diseases of the Basal Ganglia

Acute
  Hypoxia
  Hypoglycemia
  Carbon monoxide poisoning
  Hemolytic-uremic syndrome
  Other diseases
    Osmotic myelinolysis
    Encephalitis
Chronic
  Inborn errors of metabolism
    Leigh disease
    MELAS
    Glutaric acidemia type II
    Methylmalonic acidemia
    Maple syrup urine disease
    Wilson disease
  Degenerative diseases
    Juvenile Huntington disease
    Sequelae of acute insults
      Basal ganglia calcification
  Dysmyelinating diseases
    Canavan disease
    Metachromatic leukodystrophy
  Other diseases
    Neurofibromatosis type 1

Note.—MELAS = mitochondrial myopathy, encephalopathy, lactic acidosis, and strokelike episodes.

throughout childhood (Figs 1, 2) (19). A similar phenomenon occurs during early adulthood in the putamen and in later adulthood in the caudate nucleus (16–19).

■ **BASAL GANGLIA PATHOLOGIC PROCESSES**

As with other diffuse conditions of the central nervous system, bilateral basal ganglia lesions frequently manifest with nonfocal clinical features ranging from increased irritability, lethargy, seizure, behavioral changes, or dystonia to more serious respiratory distress and coma. Occasionally, patients may manifest with a movement disorder such as chorea, which suggests a specific disease entity (Huntington disease), but this is uncommon. The abruptness of symptom onset, however, helps direct the differential diagnosis into two categories of disease (Table 1). The disorders that manifest short term usually result from iatrogenic

or environmental insults. The clinical histories in these children are usually necessary to determine the specific cause. Typically, these patients are well until a precipitating event or period in time.

If acute causes are eliminated, chronic processes that may involve the basal ganglia must be considered. This second group of conditions (Table 1) represent inherent biochemical or structural abnormalities within the basal ganglia that are predominantly irreversible. Children with these conditions may also present with a wide spectrum of symptoms, albeit chronic, ranging from dramatic rigidity, gait disturbance, or chorea to relatively no symptoms. Movement disorders are more commonly seen in these patients. Furthermore, the size of the basal ganglia lesions does not necessarily correlate with the severity of the clinical findings.

Of course, substantial overlap exists between acute and chronic processes. Acute injuries may result in permanent basal ganglia damage, and chronic processes may manifest acute exacerbations or be superimposed with acute toxicities.

The following discussion is concerned with the differential clinical and radiologic features of diffuse basal ganglia abnormalities of childhood. We suggest a simplified approach to these lesions in the pediatric patient based on the clinical presentation of acute versus chronic symptoms (Table 1).

● **Acute Conditions**
The basal ganglia are prone to injury by any insult that decreases the availability of ATP. The neuronal damage results from disruption of the ATP-dependent sodium-potassium pump and the ion gradients that it regulates. The intracellular retention of sodium leads to an increase in intracellular water and cytotoxic edema. The depletion of ATP also results in the extracellular accumulation of glutamate, the main neurotransmitter of cortical nerve fibers. Glutamate is a potent excitotoxin, which, through its actions on N-methyl-D-aspartate receptors, results in the intracellu-
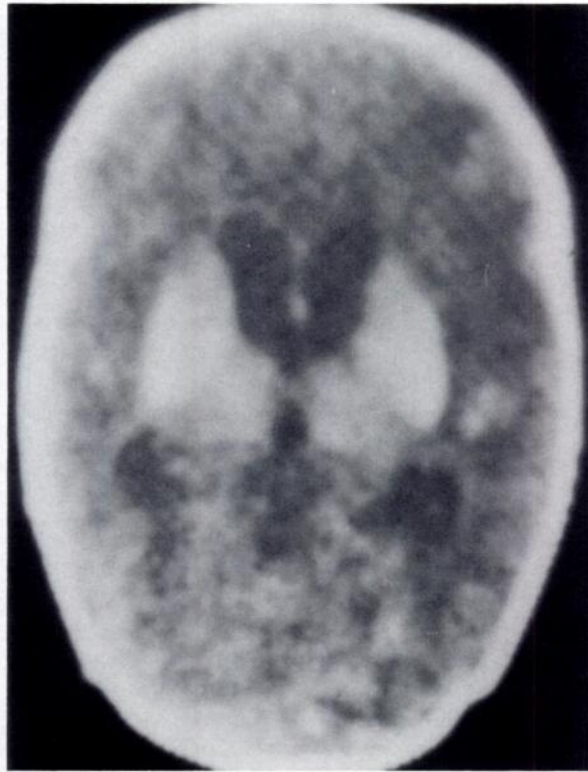
5a.

5b.
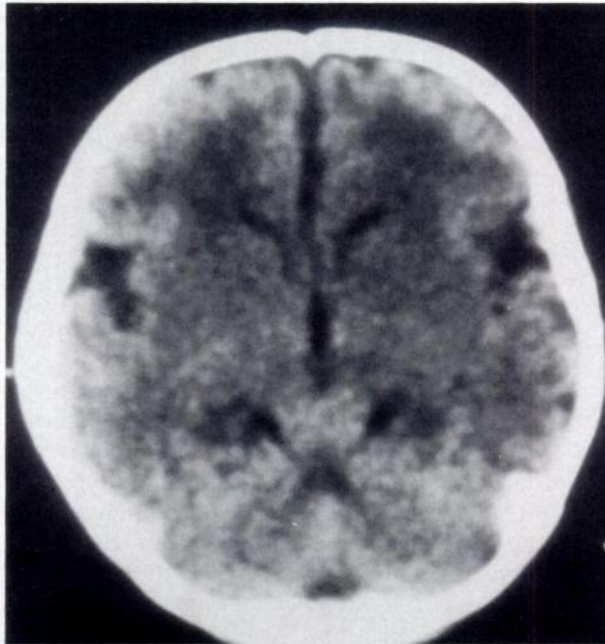
6a.

6b.

Figures 5, 6. Hypoxia. **(5a)** Unenhanced axial computed tomographic (CT) scan of a 4-month-old boy, obtained immediately after a witnessed episode of respiratory arrest, reveals hemorrhagic infarction of the basal ganglia and thalami on a background of diffuse cerebral edema. **(5b)** Unenhanced axial CT scan obtained 1 month later demonstrates profound cystic encephalomalacia to include the basal ganglia, reflecting the severity of the hypoxic damage. Note bilateral basal ganglia calcifications. **(6a)** Unenhanced axial CT scan of a 7-day-old full-term newborn who experienced perinatal asphyxia shows diffuse low attenuation within the basal ganglia. **(6b)** Unenhanced axial CT scan obtained at follow-up 4 years later demonstrates atrophy of the basal ganglia, which is most dramatic in the putamina.
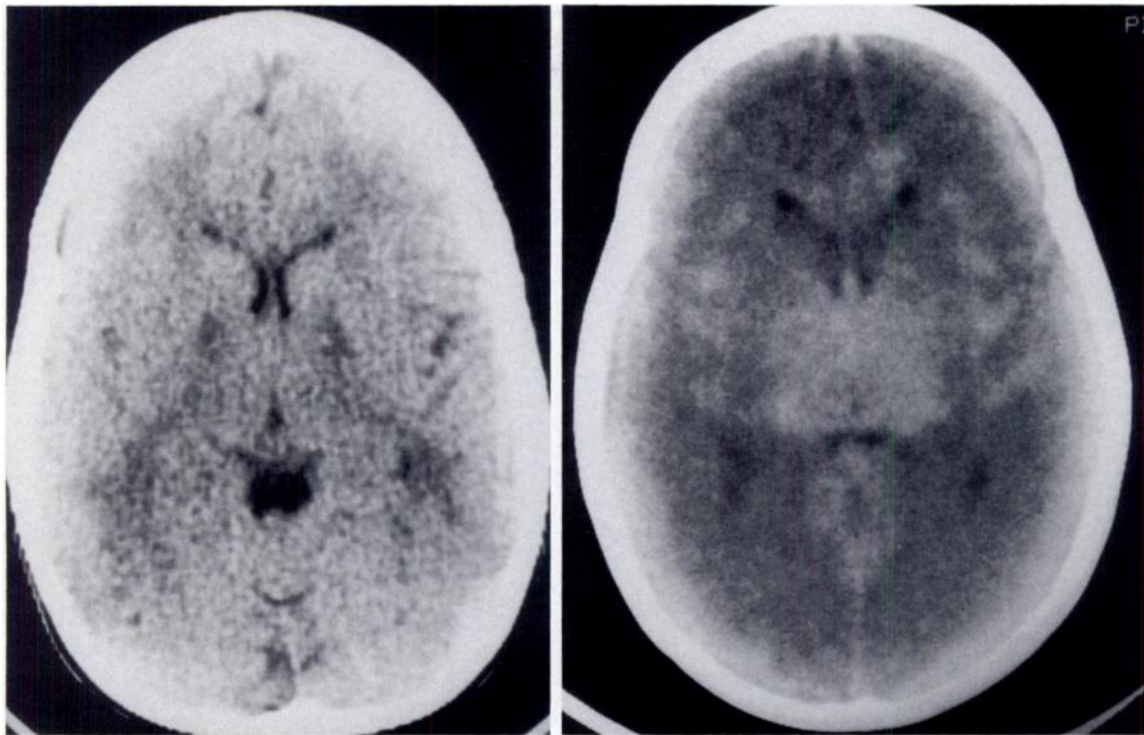
7.   **8.**

Figures 7, 8. (7) Hypoxia from near drowning. Unenhanced axial CT scan of a 5-year-old boy who was found submerged in the bathtub, blue and breathless, shows symmetric areas of low attenuation in the globi pallidi. The boy was successfully resuscitated by his mother. (8) Hypoxia from child abuse (strangulation). Unenhanced axial CT scan of a toddler who ultimately died demonstrates the "CT reversal sign," which refers to the pattern of diffusely decreased attenuation of the cerebral gray and white matter, with loss of the normal gray-white matter differentiation. The peripheral cerebral area of relative low attenuation accentuates the higher attenuation of the less involved central nuclei—in this case, the thalami. The basal ganglia are not always as involved and may retain their attenuation on CT scans; however, in this case, they appear as areas of low attenuation.

lar influx of calcium. The intracellular increase in calcium, in turn, initiates a series of degradative enzymatic cascades that lead to free radical formation, lipid peroxidation, and ultimately cell death. The basal ganglia, which are richly innervated by the cerebral cortex, contain high concentrations of glutamate and a large number of N-methyl-D-aspartate receptors (4–11).

Hypoxia.—Any process that diminishes ATP production can lead to basal ganglia damage (4–9,11). The acute deprivation of oxygen (hypoxia) results in the redirection of glucose metabolism toward anaerobic pathways for energy production (Fig 3). Anaerobic respiration produces inadequate amounts of ATP and inflicts further cellular damage by creating lactic acidosis. Lactic acidosis alters the intracellular environment and uncouples metabolic activity. Hypoxia, whether secondary to respiratory arrest (Figs 5a, 6a), near drowning

(Fig 7), or strangling (Fig 8), will result in diffuse basal ganglia injury (10,20–24). If hypoxic damage is extensive, the CT reversal sign (Fig 8) may be seen, which has a poor prognosis and indicates irreversible brain damage (20,21).

Hypoglycemia.—Hypoglycemia has also been reported to have manifestations analogous to those of hypoxia (25–29). The absence of glucose, like that of oxygen, uncouples the normal cerebral metabolism. Although the mechanism for injury may be slightly different, as lactic acidosis does not occur in hypoglycemia, the final pathway of decreased ATP is similar. Hemorrhage, which may be seen with hypoxic damage, however, is rarely seen with hypoglycemic damage (26).
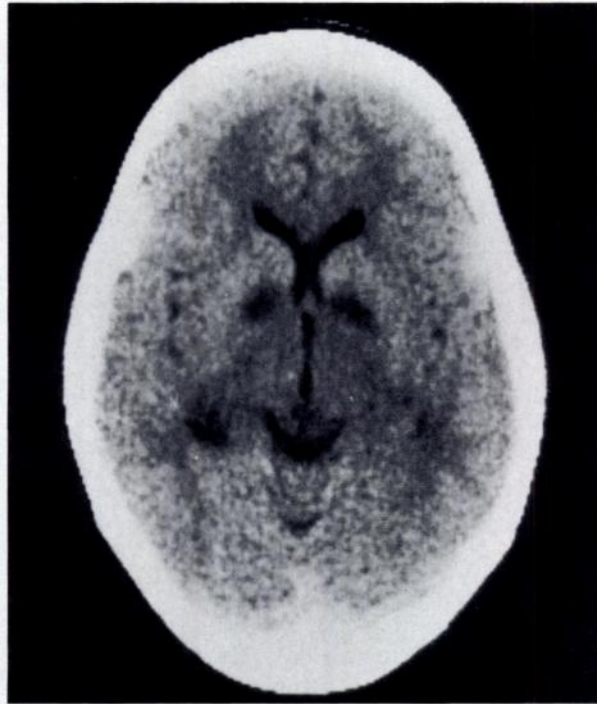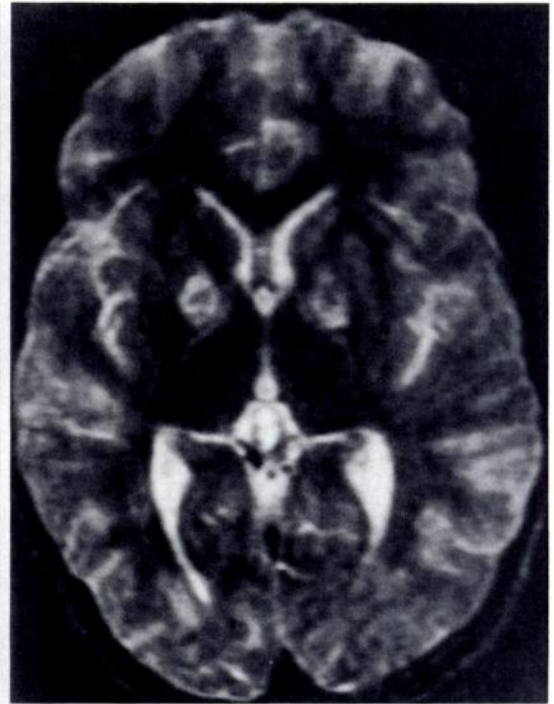
9.   **10.**

Figures 9, 10.   Carbon monoxide poisoning. **(9)** Unenhanced axial CT scan of a lethargic 6-year-old child whose home had a charcoal heater demonstrates low-attenuation lesions of the globi pallidi, typical with this type of toxicity. (Image courtesy of James G. Smirniotopoulos, MD, Department of Radiologic Pathology, Armed Forces Institute of Pathology, Washington, DC.) **(10)** Axial T2-weighted MR image of an adolescent girl who was somnolent and unresponsive from gas fumes in an enclosed garage depicts high-signal-intensity lesions in the globi pallidi and, to a lesser degree, in the caudate nuclei and putamina.

Carbon Monoxide Poisoning.—Oxygen delivery to the basal ganglia can also be reduced after carbon monoxide poisoning. The three proposed mechanisms for carbon monoxide toxicity are its (*a*) competitive binding to hemoglobin, decreasing the availability of oxyhemoglobin; (*b*) shifting of the oxyhemoglobin dissociation curve to the left, decreasing the oxygen release in tissue; and (*c*) direct toxicity on mitochondria through binding to cytochrome a_3 (30,31). It is interesting that carbon monoxide preferentially affects the

globus pallidus (Figs 9, 10) but may affect the remainder of the basal ganglia (Fig 10) and cerebral white matter. The prognosis, however, correlates more with the degree of white matter injury and not the extent of pallidal damage (30).

Hemolytic-Uremic Syndrome.—Oxygen (and glucose) delivery to the basal ganglia is also disrupted by vascular occlusion. Hemolytic-uremic syndrome is an uncommon multisystem disorder associated with microthrombosis of the basal ganglia (Fig 11a). This syndrome is characterized by microangiopathic hemolytic anemia, acute renal failure, thrombocytopenia, and microthrombosis.
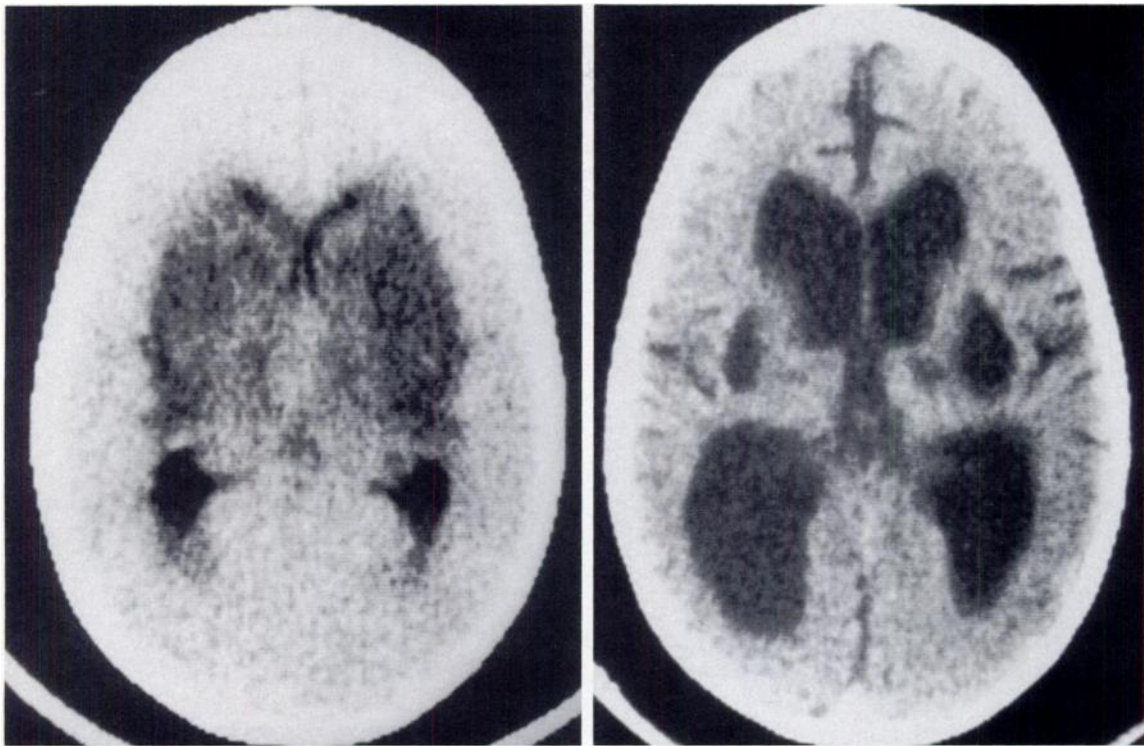
a.   **b.**

Figure 11. Microthrombosis as a result of hemolytic-uremic syndrome. (a) Unenhanced axial CT scan of a 1-year-old comatose girl reveals symmetric areas of low attenuation throughout the basal ganglia and thalami. (b) Unenhanced axial CT scan obtained 6 months later demonstrates atrophy of the caudate, with cystic encephalomalacia of the putamina, globi pallidi, and thalami.

Most patients are younger than age 5 years. Neurologic complications have been reported in 20%–50% of patients. Microthrombosis of the basal ganglia, thalami, hippocampi, and cortex may occur. Large vessel thrombi have also been reported (32).

The basic mechanism for acute cellular damage by hypoxia, hypoglycemia, carbon monoxide poisoning, and hemolytic-uremic syndrome is similar in that all result in a decreased level of ATP. The clinical features may, therefore, mimic one another. The severity of symptoms depends on the extent of exposure to the insult and ranges from mild lethargy and weakness to coma or even death.

One can determine the underlying cause for the injury only by taking a careful clinical history.

Other Diseases.—The basal ganglia, probably because of their metabolism, are also very sensitive to electrolyte imbalances. In particular, the rapid correction of sodium can result in osmotic myelinolysis (central pontine and extrapontine myelinolysis). Typically, the central pons (Fig 12a) is affected, but the basal ganglia (Fig 12b), thalami, and other ex-

a.

b.

c.
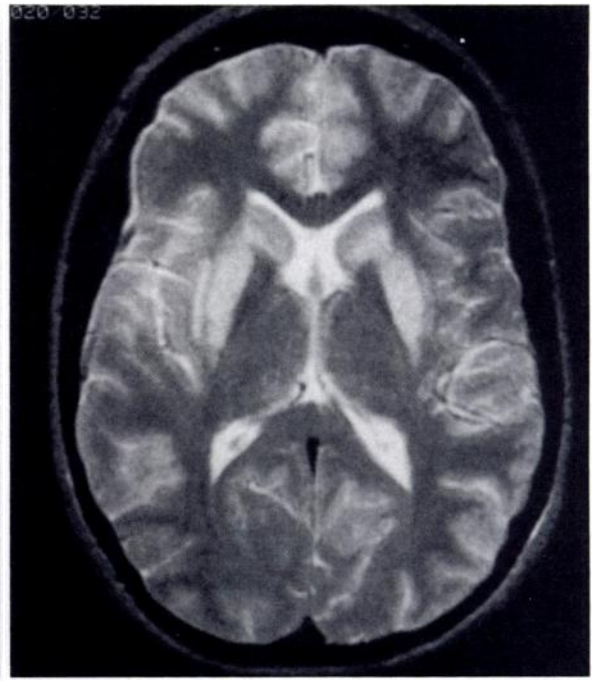
Figure 12. Osmotic myelinolysis. Axial T2-weighted MR images of a dehydrated teenaged girl (initial sodium level, 105 mmol/dL), who was administered vigorous fluid and sodium correction therapy, reveal high-signal-intensity lesions in the pons (**a**, central pontine myelinolysis) and basal ganglia (**b**, extrapontine myelinolysis). Although her condition initially improved after rehydration, within 2 weeks, her neurologic course progressed to a pseudocoma state ("locked-in" syndrome). After conservative management and rehabilitation, she recovered completely. (**c**) Axial T2-weighted MR image obtained 4 months later shows resolution of the basal ganglia lesions.
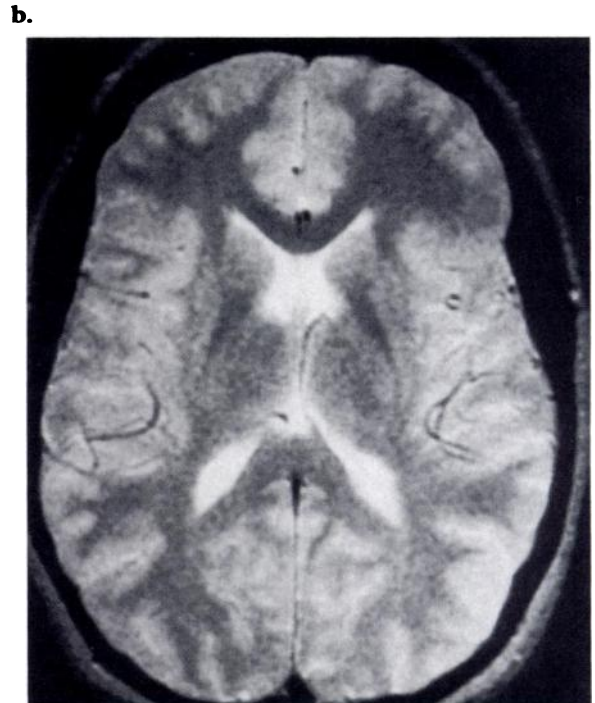
trapontine locations may also be involved. Isolated extrapontine myelinolysis has also been reported (33–38).

In osmotic myelinolysis, there is preferential loss of myelin with relative preservation of neurons and axons. Norenberg et al (37) postulated that the mixture of gray and white matter in the affected regions accounts for its distribution. The rapid correction of sodium in some way results in the release of myelinotoxic compounds by the gray matter components. The lack of involvement of regions consisting of predominantly white matter, such as the internal capsule, or predominantly gray matter, such as cerebral cortex in osmotic myelinolysis, supports this theory (33–38).

This entity was first reported in malnourished alcoholic adults (35) but has also been reported in children and adolescents (33,34). Neurologic manifestations include spastic quadriparesis and pseudobulbar palsy, with

progression in 3–5 days to pseudocoma (locked-in syndrome). Although death is a common feature, survival beyond 6 months can be seen in up to 10%. If recovery from osmotic myelinolysis occurs, the extrapontine lesions resolve first (Fig 12c) (33). When osmotic myelinolysis occurs and the patient dies, it is from a secondary complicating illness, usually respiratory (34–38).

Diffuse cerebral encephalitis results when organisms, usually viral agents, overwhelm
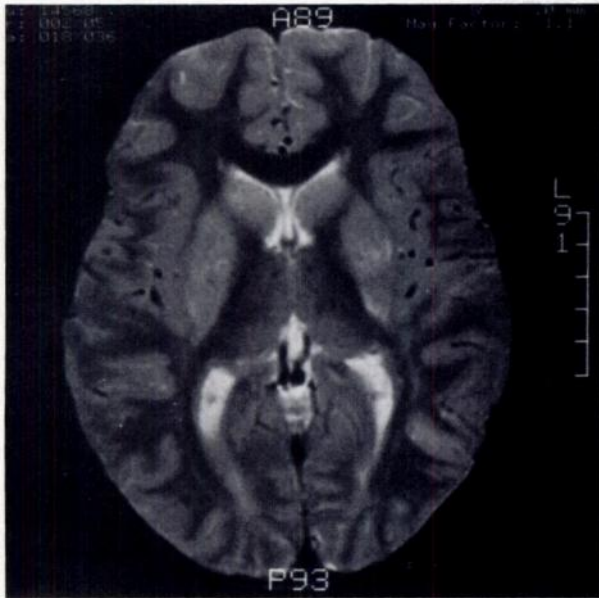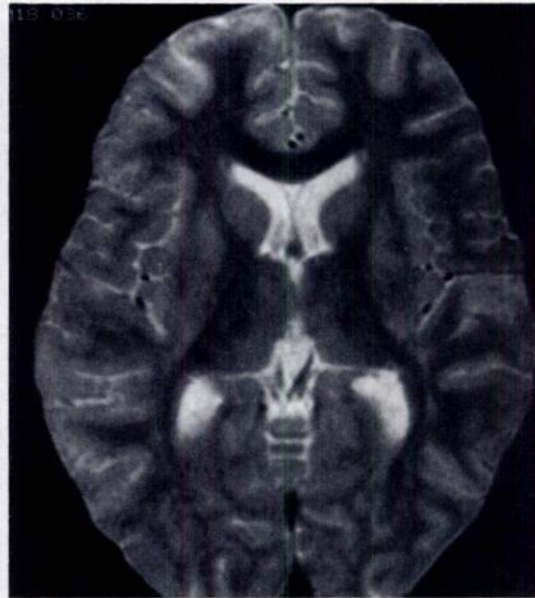
13a. **13b.**

14a. **14b.**

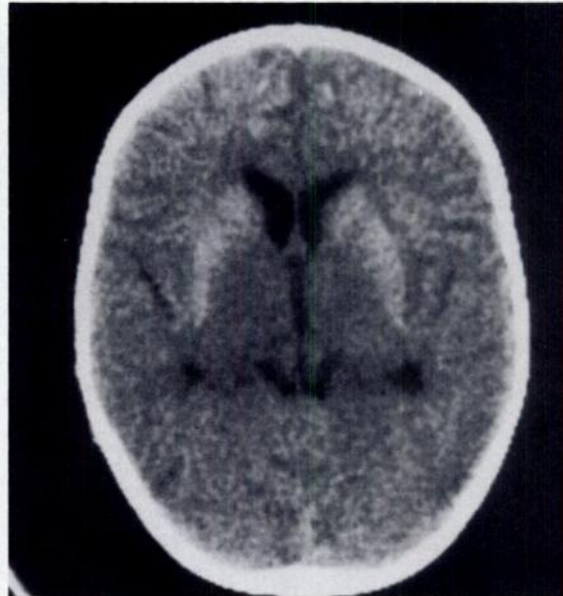**Figures 13, 14.** Encephalitis. **(13a)** Initial axial T2-weighted MR image of a 3½-year-old child with a 2-day history of fever and vomiting associated with a 45-minute seizure reveals bilateral hyperintense basal ganglia lesions. After administration of acyclovir, the child fully recovered. **(13b)** Axial T2-weighted MR image obtained 1 week later demonstrates almost complete resolution of the basal ganglia lesions. **(14a)** Unenhanced axial CT scan of a 1½-year-old child with fever, who, according to a measurement of cerebrospinal fluid viral titers was found to have eastern equine encephalitis, reveals symmetric hemorrhagic infarction of the caudate nuclei and putamina. **(14b)** Subsequent unenhanced axial CT scan obtained 2 weeks later shows progression of the condition.

the host defenses. The richly vascularized basal ganglia, with their end-vessel vascular supply, are prone to infections carried in the blood. Patients typically present with headache, lethargy, vomiting, anorexia, and seizure. Fever may or may not be present. The basal ganglia may be involved with transient findings (Fig 13). However, encephalitis may also result in vascular compromise, hypoxic damage, and subsequent hemorrhagic infarction (Fig 14) (39–41).

Methanol (42), cyanide (43), and hydrogen sulfide (44) poisoning have also been reported to preferentially affect the basal ganglia in adults, but their occurrence in children is rare.

a.   **b.**
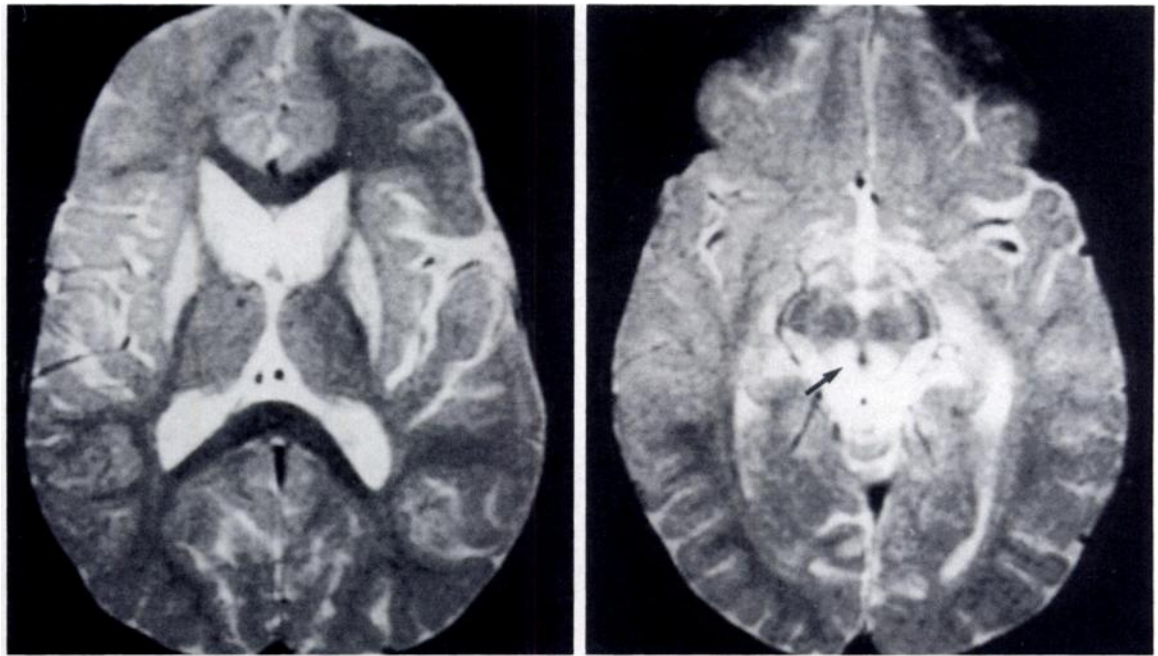
Figure 15. Leigh disease. T2-weighted MR images of an 18-month-old boy with developmental delay and lactic acidosis reveal symmetric involvement of the caudate nuclei and putamina (**a**) and the tegmentum (**b**, arrow).

● Chronic Conditions

Inherited or acquired (sequelae of acute disorders) conditions may result in long-term abnormalities of the basal ganglia. These diseases represent inherently abnormal biochemical or structural processes within the basal ganglia. Thus, the elimination of acute causes of basal ganglia abnormality suggests little hope for clinical improvement. Recognition of these chronic disorders is important for counseling purposes because most have specific patterns of inheritance.

Inborn Errors of Metabolism.—Leigh disease (subacute necrotizing encephalomyelopathy) is the prototypic metabolic disease that involves the basal ganglia. Leigh disease is an autosomal recessive biochemical disorder characterized by deficiencies in pyruvate carboxylase, pyruvate dehydrogenase complex, or cytochrome *c* oxidase (Fig 3). These enzyme deficiencies result in abnormal pyruvate metabolism with redirection of ATP production to anaerobic mechanisms. Children with Leigh disease have lactic acidosis with elevated cerebrospinal fluid and serum lactate to pyruvate ratios. Patients are typically healthy

at birth but develop progressive spasticity and dystonia with episodic neurologic and respiratory exacerbations. Leigh disease has a propensity to involve the putamina but may also affect the other basal ganglia (Figs 15a, 16) as well as the thalami, brain stem (Fig 15b), and, less commonly, white matter (Fig 16) (11,15, 45–47).

A number of other enzyme deficiencies or mitochondrial defects—probably, a variation of Leigh disease—can also lead to abnormal pyruvate metabolism and lactic acidosis with basal ganglia manifestations, particularly in the globi pallidi (Fig 17). These disorders, including Leigh disease, are part of a broader category—the lactic acidemias (11).

The mitochondrial cytopathies represent a peculiar subset of the lactic acidemias, typified by structurally abnormal mitochondria that are identified as "ragged red" fibers in a muscle biopsy specimen. Mitochondrial myopathy, encephalopathy, lactic acidosis, and strokelike episodes; mitochondrial encephalopathy with ragged red fibers; and Kearns-Sayre syndrome are the three clinical forms of mitochondrial cytopathy (48–50).
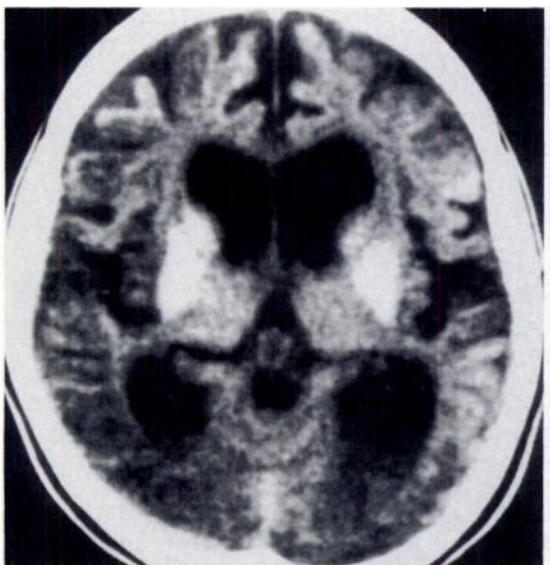
Mitochondrial myopathy, encephalopathy, lactic acidosis, and strokelike episodes make up a distinct syndrome that commonly affects the basal ganglia. This syndrome is character-
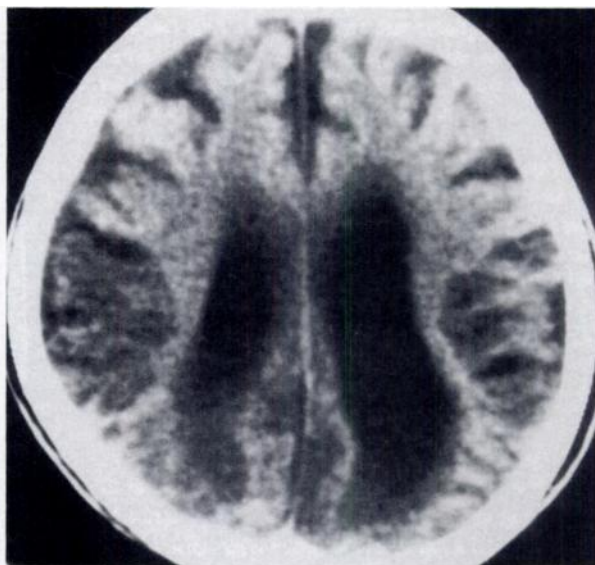
16.   **17.**

18a.   **18b.**

Figures 16–18. (16) Leigh disease. Axial T2-weighted MR image of a 7-year-old child with a long history of seizure, developmental delay, lactic acidosis, and dystonia reveals abnormal hyperintense signal intensity in the basal ganglia, thalami, and subcortical white matter. (17) Lactic acidemia. T2-weighted MR image of a 7-month-old infant with developmental delay reveals a diffusely abnormal pattern of myelination and mildly high-signal-intensity lesions of the globi pallidi (arrow). (18) Mitochondrial myopathy, encephalopathy, lactic acidosis, and strokelike episodes. Unenhanced axial CT scans of a 6-year-old girl with a long history of mental retardation, lactic acidosis, ataxia, and recurrent strokelike episodes reveal calcified basal ganglia infarcts (a) and extensive cerebral atrophy secondary to previous infarctions of the parietal, occipital, and frontal lobes (b).

ized by normal early development, short stature, lactic acidosis, seizures, and stroke. Infarction of the basal ganglia and cortical regions (Fig 18) is a hallmark radiologic feature of the syndrome. Cortical infarction predominantly occurs in the parietal and occipital regions and results in blindness. The basal ganglia infarctions commonly calcify (47–50).
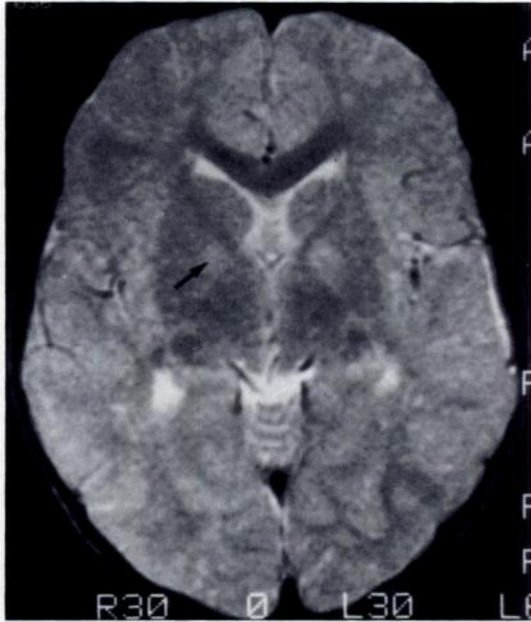
19a.
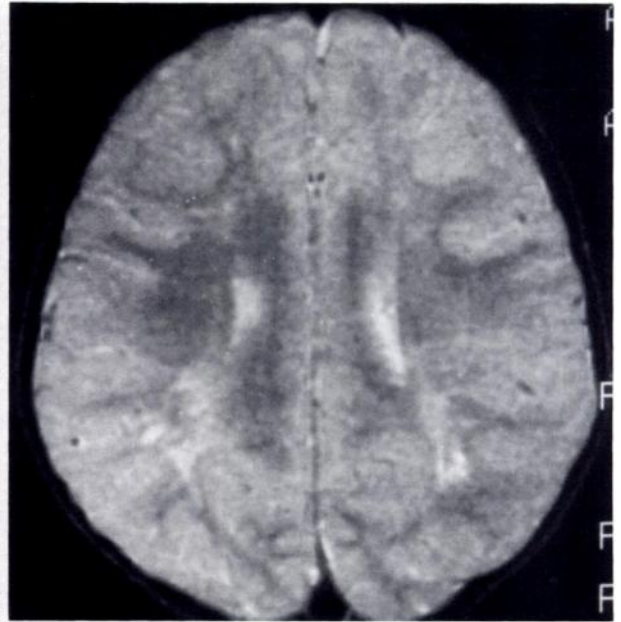
19b.

Figures 19, 20. (19) Glutaric acidemia type II.
Axial T2-weighted MR images of a 2-year-old child
with developmental delay, acidosis, and a sweaty
feet odor show subtle bilateral globi pallidi hyperin-
tensity (a, arrow) and more apparent abnormal hy-
perintense white matter (b). (20) Methylmalonic
acidemia. Axial T2-weighted MR image of a 16-year-
old boy with a broad-based gait and a history of sei-
zure activity since birth shows symmetric high-sig-
nal-intensity lesions of the globi pallidi. During the
1st week of life, he presented with lethargy, poor
feeding, and seizures. Biochemical analysis was used
to make the diagnosis.
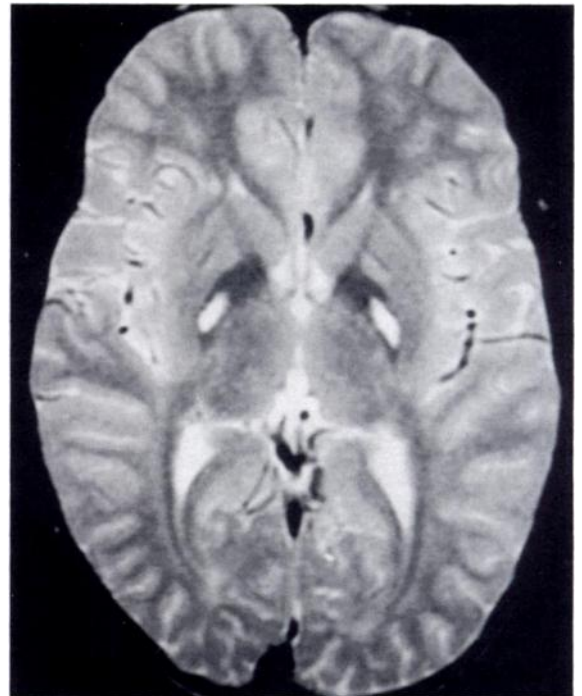
20.

Pyruvate is not the only energy substrate
used by the mitochondria for ATP production.
Amino acids and fatty acids are also funneled
into the citric acid cycle after enzymatic degra-
dation. A host of other metabolic conditions
(glutaric acidemia type II, methylmalonic aci-
demia, propionic acidemia, and maple syrup
urine disease) may alter the catabolism of
fatty acids or amino acids (Fig 3). Disruption
of these alternate routes for energy substrate
may also result in basal ganglia injury.

Glutaric acidemia type II (multiple acyl co-
enzyme A [CoA] dehydrogenase deficiency) is
an autosomal recessive disorder that typically
manifests during childhood with a glutaric
acidemia. These patients have an abnormality
in flavoprotein, which is necessary for oxidative
phosphorylation and for fatty acid catabolism.
Pathologically, this disorder is characterized
by fatty degeneration of the liver, cardiomyop-
athy, and renal dysplasia. Clinically, patients
are hypotonic and have a characteristic "sweaty
feet" odor. Lesions of the globus pallidus and
the white matter may be seen (Fig 19) (11).
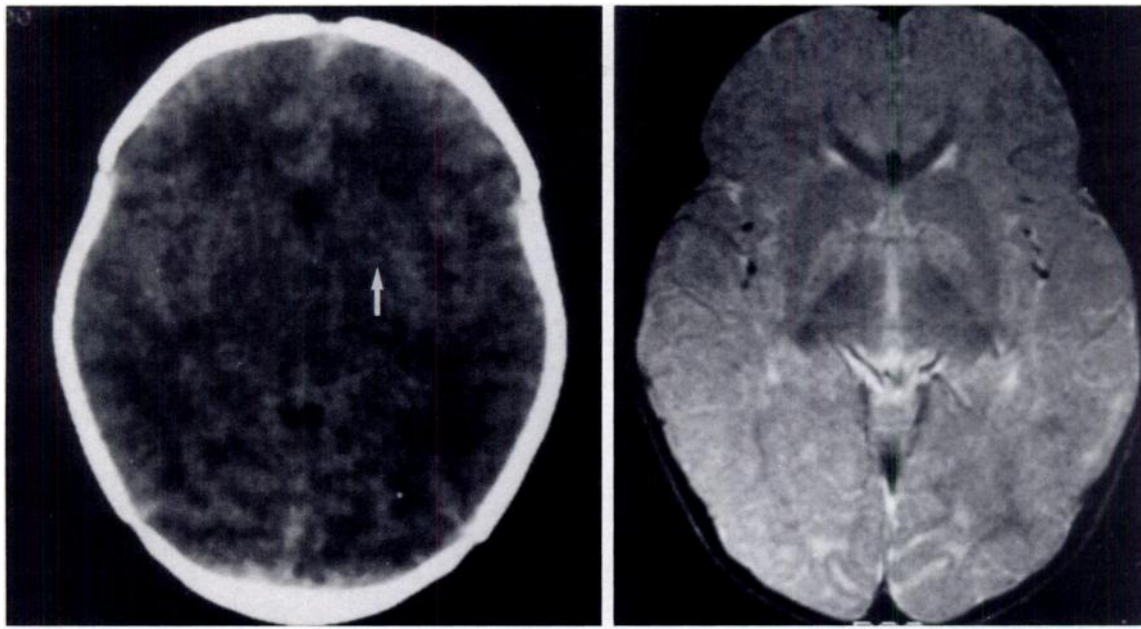
b.

Figure 21. Maple syrup urine disease. **(a)** Unenhanced axial CT scan of a child with recurrent episodes of metabolic acidosis and lethargy since the 8th day of life reveals low attenuation within the globi pallidi (arrow) and possibly the thalami, with small ventricles suggesting generalized edema. The scan was obtained when the child was 5 months old and was experiencing an acute episode. **(b)** Axial T2-weighted MR image of the same child, obtained at age 17 months, reveals moderate hyperintensity of the globi pallidi.

Propionyl CoA and methylmalonyl CoA are important intermediaries in the catabolism of several essential amino (isoleucine, valine, methionine, threonine, thymine) and fatty acids. Deficiencies in propionyl-CoA carboxylase or methylmalonyl-CoA mutase result in propionic and methylmalonic acidemia, respectively. Patients present with ketoacidosis, hypotonia, developmental delay, dehydration, seizure, and lethargy. Basal ganglia injury, although more commonly seen in methylmalonic acidemia (Fig 20), may occur with either disease (11,15,47).

Maple syrup urine disease results from several inherited defects in branched-chain α-keto acid dehydrogenase. Patients are unable to catabolize branched-chain amino acids (leucine, isoleucine, and valine), which therefore are increased in their blood and urine. The urine has a characteristic smell for which the disorder was named. The primary therapy is a protein-restricted diet. The main radiologic feature is diffuse edema (Fig 21), especially of the cerebellar white matter, dorsal brain stem, cerebral peduncles, and dorsal

limb of the internal capsule. Basal ganglia and thalamic involvement may also be seen (11, 47,51).

As mentioned earlier, the basal ganglia have high trace metal concentrations that may be toxic if excessive. Wilson disease is an autosomal recessive disorder of copper metabolism characterized by the increased deposition of copper in the brain and liver. The toxic accumulation of copper leads to cell damage in both the liver and lentiform nuclei (the lenticular nucleus comprises the putamen and globus pallidus, which are apposed in a "lens" configuration), giving it the pathologic name of "hepatolenticular degeneration." Laboratory tests reveal decreased levels of total serum copper and ceruloplasmin and increased urinary copper excretion. Symptoms referable to liver failure usually predate neurologic symptoms. Liver biopsy will help confirm the diagnosis. Treatment consists primarily of copper chelation with penicillamine. Lesions
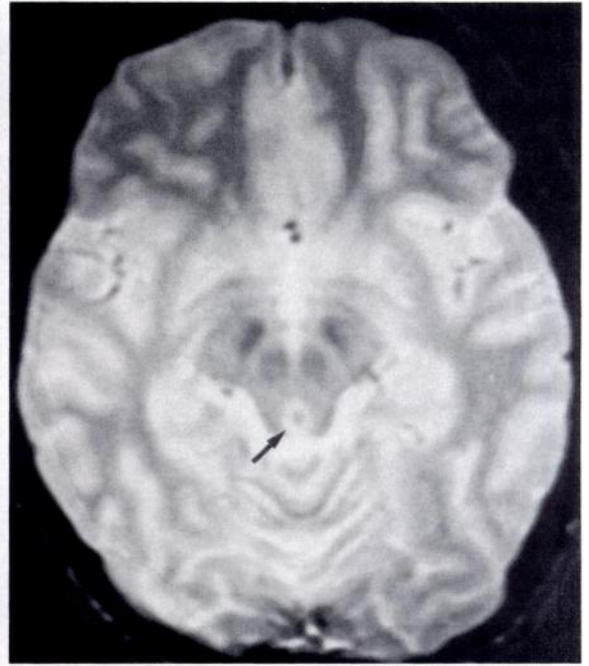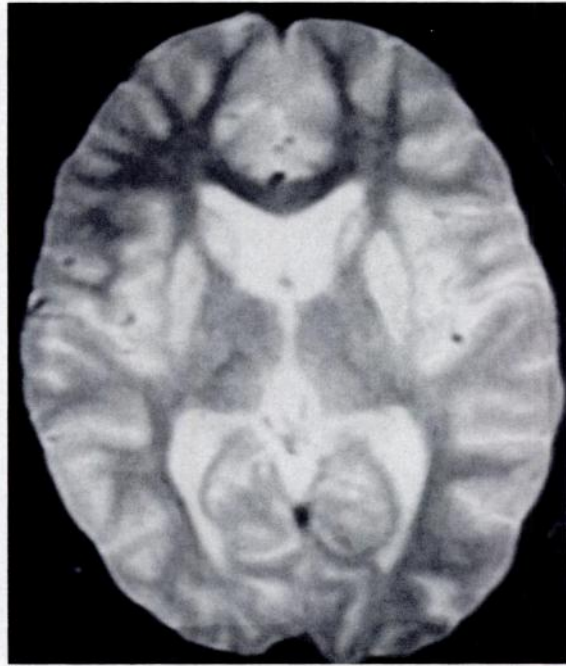
a.   **b.**

Figure 22. Wilson disease. Axial T2-weighted MR images of a 14-year-old adolescent with slowly progressing dysphagia, dysphonia, dysarthria, and tremor reveal bilateral symmetric lesions of the caudate nuclei and putamina (a) and the periaqueductal region (b, arrow) in association with mild cerebral atrophy. Findings from a liver biopsy that was performed when the child was 7 years old were used for diagnosis.

Figure 23. Juvenile Huntington disease. Unenhanced axial CT scan of a 7-year-old boy with rigidity, mental retardation, dyslalia, seizures, and choreiform movements that have been progressive over the past 3 years reveals marked atrophy of the basal ganglia, most dramatically in the caudate nuclei.


of the basal ganglia, thalami, and occasionally the periaqueductal gray matter (Fig 22) are seen. The distribution of Wilson disease may mimic that of Leigh disease (compare Fig 15 with Fig 22) (52–54).

Table 2
Conditions Associated with Basal Ganglia Calcification

Endocrine
    Hypoparathyroidism
    Pseudohypoparathyroidism
    Pseudopseudohypoparathyroidism
    Hyperparathyroidism
    Hypothyroidism
Metabolic
    Leigh disease
    Mitochondrial cytopathy
    Fahr disease (familial cerebrovascular ferro-
        calcinosis)
Congenital or developmental
    Familial idiopathic symmetric basal ganglia
        calcification
    Hastings-James syndrome
    Cockayne syndrome
    Lipoid proteinosis (hyalinosis cutis)
    Neurofibromatosis
    Tuberous sclerosis
    Oculocraniosomatic disease
    Methemoglobinopathy
    Down syndrome
Inflammatory
    Toxoplasmosis
    Congenital rubella
    Cytomegalovirus
    Measles
    Chicken pox
    Pertussis
    Coxsackie B virus
    Cysticercosis
    Systemic lupus erythematosus
    Acquired immunodeficiency syndrome
Toxic
    Hypoxia
    Cardiovascular event
    Carbon monoxide intoxication
    Lead intoxication
    Radiation therapy
    Methotrexate therapy
    Nephrotic syndrome

Degenerative Diseases.—Huntington disease is the classic degenerative disease of the basal ganglia. Recent studies, however, have linked Huntington disease to abnormalities in oxidative phosphorylation and glutamate regulation, suggesting that it represents an inborn error of metabolism (55–57). In any case, Huntington disease is an autosomal dominant disorder; it may manifest during childhood or adolescence. The patients typically present with rigidity, dyslalia, seizures, and mental deterioration. Chorea is usually present but is more commonly a late feature. Pathologically, there is diffuse cerebral atrophy, particularly of the caudate and putamen (Fig 23) (11,15,58,59).

Acute insults to the basal ganglia may be sufficiently extensive to cause irreversible damage that can be detected radiologically. Although cystic encephalomalacia may be seen (see Figs 5b, 6b, 11b), more commonly dystrophic calcification is present. Calcification is probably the most common abnormality of the basal ganglia seen in children, with a reported prevalence of 1.1%–1.6% (60,61). Although basal ganglia calcification may be "normal" and inconsequential in adults, this finding in a child is important and serves as a marker of more extensive brain damage (60). Unfortunately, basal ganglia calcifications are not specific for any given disease and can be associated with a number of conditions (Table 2) (60–63).
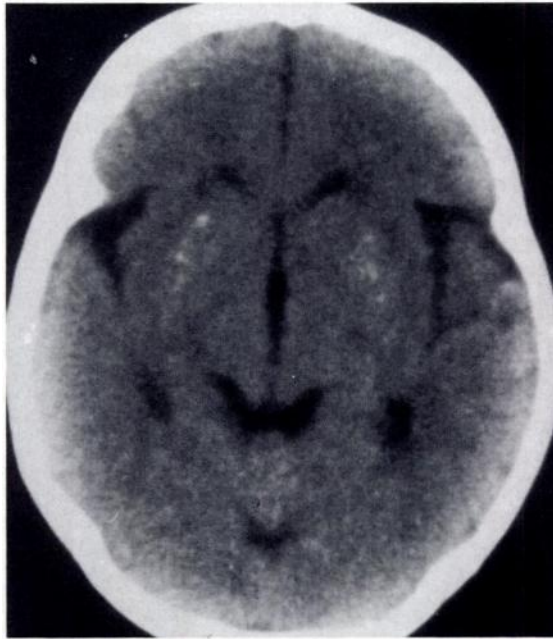
24.
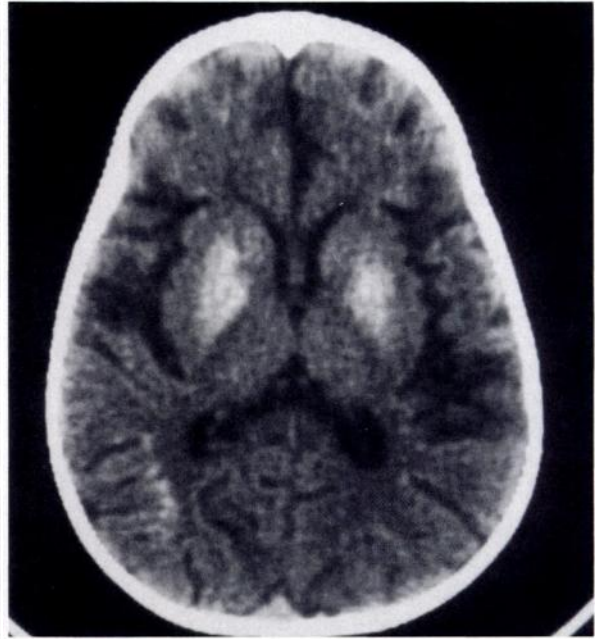
25.
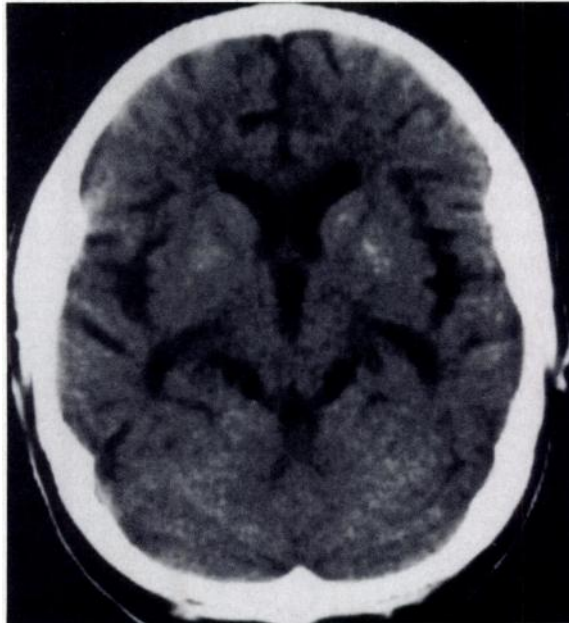
26.
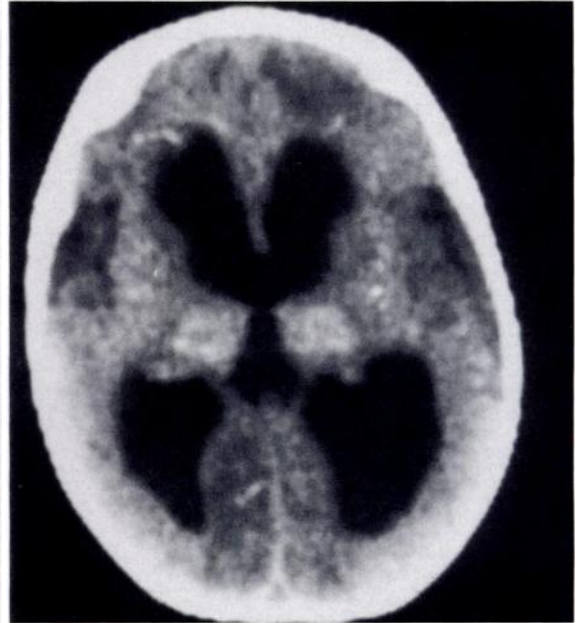
27.

Figures 24–27. Basal ganglia calcification. Unenhanced axial CT scans reveal calcifications in a case of congenital cytomegalovirus in a 7-month-old infant **(24)**, congenital acquired immunodeficiency syndrome in a 13-month-old child **(25)**, systemic lupus erythematosus in a 15-year-old adolescent **(26)**, and congenital nephrotic syndrome in a 2-month-old infant **(27)**.

Basal ganglia calcification, although best evaluated with CT (Figs 24–28), may be seen with MR imaging. The MR imaging appearance of basal ganglia calcification consists most commonly of hypointensities on T1- and T2-weighted images. Calcium has nonmobile protons that result in signal void that is more apparent on T2-weighted MR images. Occasionally, calcifications may appear hyperin-

tense on T1-weighted MR images and hypointense on T2-weighted images (Fig 28). The T1 shortening in these cases is believed to be related to a variation in the crystalline structure of the calcifications (64).

Dysmyelinating Diseases.—Although generally considered gray matter nuclei, the basal ganglia are a mixture of gray and white matter

a.   **b.**   **c.**

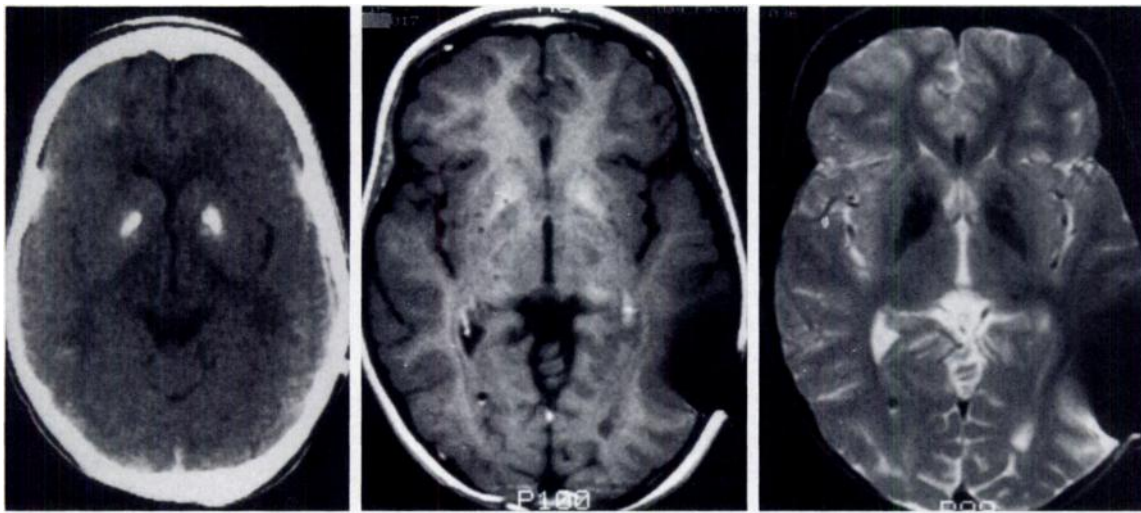**Figure 28.** Basal ganglia calcification. (a) Unenhanced axial CT scan of a patient who developed mineralizing microangiopathy after radiation therapy and intrathecal chemotherapy for a medulloblastoma shows calcification. Axial T1-weighted (b) and T2-weighted (c) MR images show the calcification as hyperintense and hypointense, respectively.

elements that collectively contribute to the MR signal intensity of the basal ganglia. Abnormalities of white matter elements may also result in abnormal MR imaging signal intensity in the basal ganglia. It is important to note that basal ganglia lesions may result from diseases unrelated to oxidative phosphorylation.

Under normal circumstances, the signal intensity contributions of the myelin are dwarfed by those of the neuronal elements, as the MR imaging appearance of the basal ganglia parrots that of the peripheral gray matter (see Figs 1, 2). Under pathologic conditions, however, the abnormal myelin may alter the MR imaging signal intensity characteristics of the basal ganglia. Osmotic myelinolysis (Fig 12) is an example of such an acute condition. Chronic diseases of myelination (Canavan disease, metachromatic leukodystrophy) may also affect the appearance of basal ganglia. These abnormalities of myelin are best appreciated as regions of abnormal hyperintensity on T2-weighted images. Although the white matter changes are the dominant radiologic feature of these disorders, the involvement of the myelin elements of the basal ganglia is important to recognize and not to be misconstrued as a second process.

Canavan disease (spongiform leukodystrophy) is an autosomal recessive disorder of infancy with higher frequency in Ashkenazi Jews. Patients usually present during the 1st year of life with megalencephaly, hypotonia, and failure to thrive. Seizures, spasticity, and blindness may follow, with death occurring usually by the age of 5 years. The disease diffusely involves the white matter but may also affect the basal ganglia (Fig 29) (15,65,66).

Metachromatic leukodystrophy is an autosomal recessive dysmyelinating disorder that can manifest in infancy or adulthood. It is characterized by gait disorder, tremor, and strabismus early, with progressive intellectual decline. The disease results from a deficiency in arylsulfatase A, an enzyme that is crucial to normal myelination. MR imaging reveals abnormally lengthened T2 signal intensity in the white matter tracts and occasionally in the basal ganglia (Fig 30) (15,66).

Other Diseases.—"Unidentified bright objects" may occur in the basal ganglia of patients with neurofibromatosis type 1, an autosomal dominant disorder with a high rate of spontaneous mutation and a reported prevalence of one in 2,000–4,000 births. Recently, it has been genetically linked to the long arm of chromosome 17. Clinical hallmarks of neurofibromatosis type 1 include multiple neurofibromas, café-au-lait spots, Lisch nodules (pigmented iris hamartomas), axillary freckles, macrocephaly, and learning disorders. However, most of these clinical features are absent during early childhood (67–72).
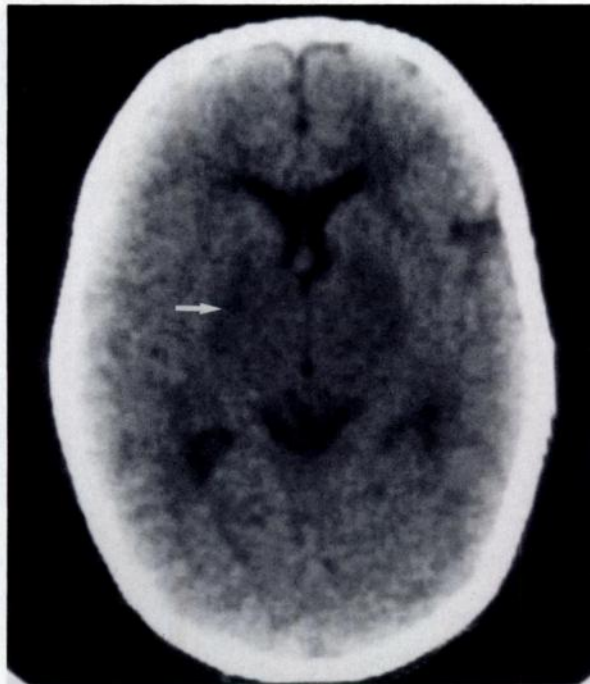
29a.
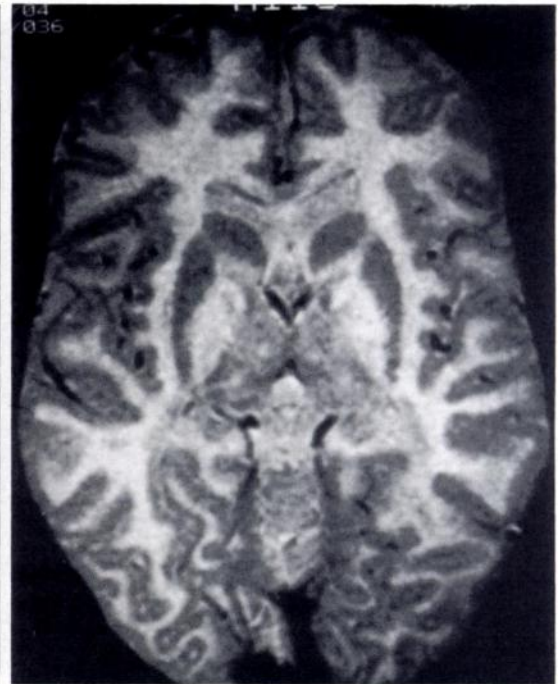
29b.

Figures 29, 30. (29) Canavan disease. (a) Unenhanced axial CT scan of a 3-month-old infant suggests low-attenuation lesions of the globi pallidi (arrow). (b) T2-weighted MR image of the same child, obtained at age 2½ years, shows diffuse, abnormal high signal intensity of the white matter and of the globi pallidi. A fibroblastic culture was used for diagnosis in this child, who has had decreased vision, developmental delay, and seizures since age 6 months. (30) Metachromatic leukodystrophy. Axial T2-weighted MR image of a 3-year-old child with developmental delay, microcephaly, spastic diplegia, and hypotonia, who was found to have deficient arylsulfatase A activity, reveals diffuse white matter hyperintensity and abnormal high signal intensity in the globi pallidi (arrow).

Because of the lack of apparent pathologic abnormality in the unidentified bright objects, these lesions have been called hamartomas. However, they have also been reported to resolve (70,71). We suggest calling them dysmyelinating lesions, as true hamartomas should remain unchanged. T2-weighted MR imaging of up to 70%–80% of asymptomatic children with neurofibromatosis type 1 reveals these hyperintense central nervous system lesions (personal observations, 1992) in the basal ganglia, most commonly in the globus pallidus (Fig 31), brain stem (Fig 32), thalamus, and cerebellar white matter. It is

30.

interesting that these lesions may also appear hyperintense on T1-weighted MR imaging (Fig 31) (72). Contrast material–enhancement of these lesions should raise suspicion for malignancy, specifically for astrocytoma, which is associated with neurofibromatosis type 1. Although less helpful, CT scans may occasionally depict these dysmyelinating lesions (Fig 33).

31a.
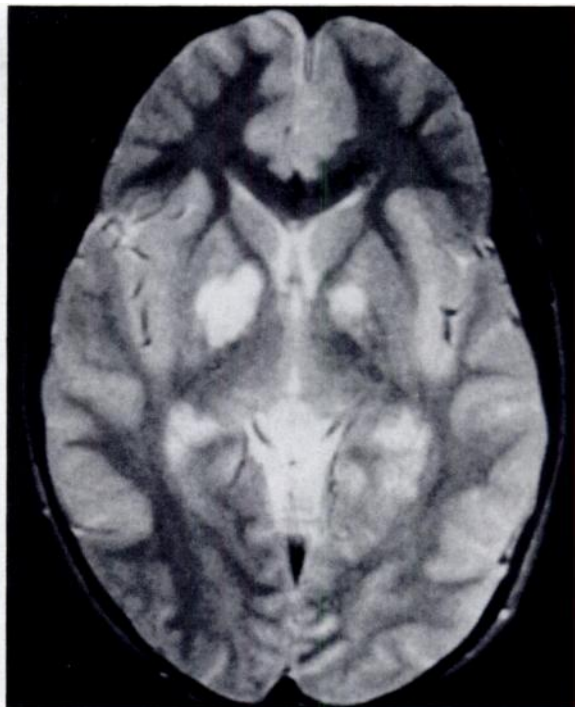
31b.

32.

Figures 31, 32. Neurofibromatosis type 1 dysmy-elinating lesions. (31) Axial T1-weighted (a) and T2-weighted (b) MR images of an 8-year-old girl show hyperintense basal ganglia abnormalities. Clinically, the findings from neurologic examination were normal. (32) Axial T2-weighted MR image of a 5-year-old boy with normal findings from neurologic examination shows hyperintense lesions in the brain stem. He had similar lesions in the basal ganglia.

pearance may be supportive of the diagnosis, however. Carbon monoxide, for example, has the propensity to affect the globus pallidus. Osmotic myelinolysis, although it may occur in purely extrapontine locations, commonly has an associated central pontine lesion.

If acute causes are eliminated, chronic processes must be considered. With these entities, the prognosis is poor, as they are invariably progressive and the damage is irreversible. The identification of the specific disease has important counseling implications, since hereditary factors are involved with most of these disorders. The general distributions are summarized in Table 3.

In Leigh disease, the lesions occur predominantly in the putamen but may also affect the caudate, globus pallidus, thalamus, brain

■ **SUMMARY**

Findings of bilateral basal ganglia lesions in a child are always significant. Acute processes that affect the basal ganglia can have similar distributions (Table 3). Usually, only after taking a thorough history can one identify the insulting agent or cause. The radiologic ap-
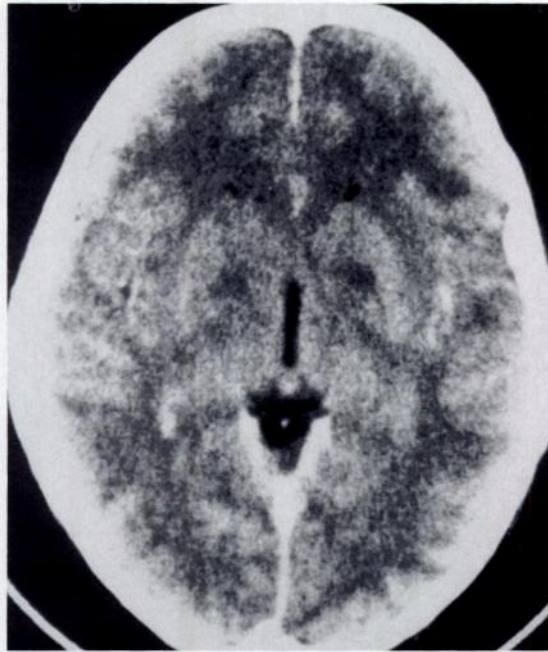
Figure 33. Neurofibromatosis type 1 dysmyelinating lesions. Unenhanced axial CT scan of a 6-year-old girl shows low-attenuation lesions in the globi pallidi.

stem, and white matter. Wilson disease may mimic Leigh disease radiologically. The clinical differentiation of Wilson disease from Leigh disease, however, should be apparent. Wilson disease usually has associated hepatic dysfunction; Leigh disease does not. The remainder of the inborn errors of metabolism primarily affect the globus pallidus, and their differentiation is based on biochemical testing.

Huntington disease is an uncommon childhood disorder that is usually only considered when a family history of the disorder is elicited. Patients with juvenile Huntington disease present more commonly with rigidity, dyslalia, mental deterioration, and seizure, but eventually most develop the more typical choreoathetoid movement disorder.

It is also important to recognize the presence of white matter elements in the basal ganglia. Both acute and chronic white matter disorders may result in basal ganglia abnormalities. Neurofibromatosis type 1 is possibly one such entity.

■ REFERENCES

1. Fahn S. Biochemistry of the basal ganglia. Adv Neurol 1976; 14:59–89.
2. Chugani HT, Phelps ME, Mazziotta JC. Positron emission tomography study of human brain functional development. Ann Neurol 1987; 22:487–497.
3. Lehninger AL. Principles of biochemistry. New York, NY: Worth, 1982; 331–559.
4. Siegel GJ, Agranoff BW, Albers RW, Molinoff PB, eds. Basic neurochemistry: molecular, cellular, and medical aspects. 4th ed. New York, NY: Raven, 1989.
5. Rothman SM, Olney JW. Glutamate and the pathophysiology of hypoxic-ischemic brain damage. Ann Neurol 1986; 19:105–111.
6. Ikeda Y, Long DM. The molecular basis of brain injury and brain edema: the role of oxygen free radicals. Neurosurgery 1990; 27: 1–11.
7. Johnston MV, Silverstein FS. New insights into mechanisms of neuronal damage in the developing brain. Pediatr Neurosci 1986; 12: 87–89.
8. Vannucci RC. Experimental biology of cerebral hypoxia-ischemia: relation to perinatal brain damage. Pediatr Res 1990; 27:317–326.
9. Hattori H, Wasterlain CG. Excitatory amino acids in the developing brain: ontogeny, plasticity, and excitotoxicity. Pediatr Neurol 1990; 6:219–228.
10. Barkovich AJ. MR and CT evaluation of profound neonatal and infantile asphyxia. AJNR 1992; 13:959–972.
11. Scriver CR, Beaudet AL, Sly WS, Valle D, eds. The metabolic basis of inherited disease. 6th ed. New York, NY: McGraw-Hill, 1989.
12. Diezel PD. Iron in the brain: a chemical and histochemical examination. In: Waelsch H, ed. Biochemistry of the developing nervous system. New York, NY: Academic Press, 1955; 145–152.
13. Hallgren B, Sourander P. The effect of age on the non-haemin iron in the human brain. J Neurochem 1958; 3:41–51.
14. Halliwell B, Gutteridge JM. Oxygen toxicity, oxygen radicals, transition metals and disease. Biochem J 1984; 219:1–14.
15. Mirowitz SA, Sartor K, Prensky AJ, Gado M, Hodges FJ. Neurodegenerative diseases of childhood: MR and CT evaluation. J Comput Assist Tomogr 1991; 15:210–222.
16. Rutledge JN, Hilal SK, Silver AJ, Defendini R, Fahn S. Study of movement disorders and brain iron by MR. AJNR 1987; 8:397–411.
17. Drayer BP. Imaging of the aging brain. I. Normal findings. Radiology 1988; 166:785–796.
18. Drayer BP, Burger P, Darwin R, Riederer S, Herfkens R, Johnson GA. Magnetic resonance of brain iron. AJNR 1986; 7:373–380.
19. Aoki S, Okada Y, Nishimura K, et al. Normal deposition of brain iron in childhood and adolescence: MR imaging at 1.5 T. Radiology 1989; 172:381–385.
20. Adsett DB, Fitz CR, Hill A. Hypoxic-ischemic cerebral injury in the term newborn: correlation of CT findings with neurological out-

Table 3
Anatomic Distribution of Acute and Chronic Basal Ganglia Diseases

Diagnosis	Globus Pallidus	Caudate	Putamen	White Matter
Acute				
Hypoxia	+	+	+	+
Hypoglycemia	+	+	+	+
Carbon monoxide intoxication	+ +	+	+	+
Hemolytic-uremic syndrome	+	+	+	+
Osmotic myelinolysis	+	+	+	+ +pons
Encephalitis	+	+	+	+
Chronic				
Leigh disease	+	+	+ +	+
Wilson disease	+ +	+	+ +	+
Lactic acidemia	+			+
Glutaric acidemia type II	+			+
Methylmalonic acidemia	+			+
Maple syrup urine disease	+			+
Huntington disease	+	+ +	+ +	+

Note.—Regions more commonly involved are indicated by + +.

come. Dev Med Child Neurol 1985; 27:155–160.

21. Han BK, Towbin RB, De Courten-Myers G, McLaurin R, Ball WS. Reversal sign on CT: effect of anoxic/ischemic cerebral injury in children. AJNR 1989; 10:1191–1198.

22. Kjos BO, Brant-Zawadzki M, Young RG. Early CT findings of global central nervous system hypoperfusion. AJNR 1983; 4:1043–1048.

23. Taylor SB, Quencer RM, Holzman BH, Naidich TP. Central nervous system anoxic-ischemic insult in children due to near drowning. Radiology 1985; 156:641–646.

24. Fitch SJ, Gerald B, Magill HL, Tonkin ILD. Central nervous system hypoxia in children due to near drowning. Radiology 1985; 156:647–650.

25. Kalimo H, Olsson Y. Effects of severe hypoglycemia on the human brain. Acta Neurol Scand 1980; 62:345–356.

26. Hirabayashi S, Kitahara T, Hishida T. Computed tomography in perinatal hypoxic and hypoglycemic encephalopathy with emphasis on follow-up studies. J Comput Assist Tomogr 1980; 4:451–456.

27. Kaiser MC, Pettersson H, Harwood-Nash DC, Fitz CR, Chuang S. Computed tomography of the brain in severe hypoglycemia. J Comput Assist Tomogr 1981; 5:757–759.

28. Iwai A, Sakamoto T, Kinoshita Y, Yokota J, Yoshioka, Sugimoto T. Computed tomographic imaging of the brain in after hypoglycemia coma. Neuroradiology 1987; 29:398–400.

29. Richardson ML, Kinard R, Gray MB. CT of generalized gray matter infarction due to hypoglycemia. AJNR 1981; 2:366–367.

30. Miura T, Mitomo M, Kawai R, Harada K. CT of the brain in acute carbon monoxide intoxication: characteristic features and prognosis. AJNR 1985; 6:739–742.

31. Goldbaum LR, Orellano T, Dergal E. Mechanism of the toxic action of carbon monoxide. Ann Clin Lab Sci 1976; 6:372–376.

32. Kudryk BT, Coleman JM, Murtagh FR, Arrington JA, Silbiger ML. Hemolytic uremic syndrome: MR findings of CNS complications. AJNR 1991; 12:703–704.

33. Ho VB, Fitz CR, Yoder CC, Geyer CA. Resolving MR features in osmotic myelinolysis (central pontine and extrapontine myelinolysis). AJNR 1993; 14:163–167.

34. Gocht A, Colmant HJ. Central pontine and extrapontine myelinolysis: a report of 58 cases. Clin Neuropathol 1987; 6:262–270.

35. Adams RD, Victor M, Mancall EL. Central pontine myelinolysis: a hitherto undescribed disease occurring in alcoholic and malnourished patients. Arch Neurol Psychiatry 1959; 81:154–172.

36. Messert B, Orrison WW, Hawkins MJ, Quaglieri CE. Central pontine myelinolysis: considerations on etiology, diagnosis, and treatment. Neurology 1979; 29:147–160.

37. Norenberg MD, Leslie KO, Robertson AS. Association between rise in serum sodium and central pontine myelinolysis. Ann Neurol 1982; 11:128–135.

38. Miller GM, Baker HL, Okazaki H, Whisnant JP. Central pontine myelinolysis and its imitators: MR findings. Radiology 1988; 168:795–802.

39. Tarr RW, Edwards KM, Kessler RM, Kulkarni MV. MRI of mumps encephalitis: comparison with CT evaluation. Pediatr Radiol 1987; 17:59–62.

40. Al-Mateen M, Gibbs M, Dietrich R, Mitchell WG, Menkes JH. Encephalitis lethargica-like illness in a girl with mycoplasma infection. Neurology 1988; 38:1155–1158.

41. Milton WJ, Atlas SW, Lavi E, Mollman JE. Magnetic resonance imaging of Creutzfeldt-Jacob disease. Ann Neurol 1991; 29:438–440.

42. Koopmans RA, Li DKB, Paty DW. Basal ganglia lesions in methanol poisoning: MR appearance. J Comput Assist Tomogr 1988; 12:168–170.

43. Matsuo F, Cummins JW, Anderson RE. Neurological sequelae of massive hydrogen sulfide inhalation. Arch Neurol 1979; 36:451–452.

44. Finelli PF. Changes in the basal ganglia following cyanide poisoning. J Comput Assist Tomogr 1981; 5:755–756.

45. Geyer CA, Sartor KJ, Prensky AJ, Abramson CL, Hodges FJ, Gado MH. Leigh disease (subacute necrotizing encephalomyelopathy): CT and MR in five cases. J Comput Assist Tomogr 1988; 12:40–44.

46. Medina L, Chi TL, Devivo DC, Hilal SK. MR findings in patients with subacute necrotizing encephalomyelopathy (Leigh syndrome): correlation with biochemical defect. AJNR 1990; 11:379–384.

47. Kendall BE. Disorders of lysosomes, peroxisomes, and mitochondria. AJNR 1992; 13:621–653.

48. Pavlakis SG, Phillips PC, DiMauro S, DeVivo DC, Rowland LP. Mitochondrial myopathy, encephalopathy, lactic acidosis, and stroke-like episodes: a distinctive clinical syndrome. Ann Neurol 1984; 16:481–488.

49. DiMauro S, Bonilla E, Zeviani M, Nakagawa M, DeVivo DC. Mitochondrial myopathies. Ann Neurol 1985; 17:521–538.

50. Allard JC, Tilak S, Carter AP. CT and MR of MELAS syndrome. AJNR 1988; 9:1234–1238.

51. Brismar J, Aqeel A, Brismar G, Coates R, Gascon G, Ozand P. Maple syrup urine disease: findings on CT and MR scans of the brain in 10 infants. AJNR 1990; 11:1219–1228.

52. Williams FJB, Walshe JM. Wilson's disease: an analysis of the cranial computerized tomographic appearances found in 60 patients and the changes in response to treatment with chelating agents. Brain 1981; 104:735–752.

53. Lawler GA, Pennock JM, Steiner RE, Jenkins WJ, Sherlock S, Young IR. Nuclear magnetic resonance (NMR) imaging in Wilson disease. J Comput Assist Tomogr 1983; 7:1–8.

54. Aisen AM, Martel W, Gabrielsen TO, et al. Wilson disease of the brain: MR imaging. Radiology 1985; 157:137–141.

55. Perry TL, Hansen S. What excitotoxin kills striatal neurons in Huntington's disease: clues from neurochemical studies. Neurology 1990; 40:20–24.

56. Parker WD, Boyson SJ, Luder AS, Parks JK. Evidence for a defect in NADH:ubiquinone oxidoreductase (complex 1) in Huntington's disease. Neurology 1990; 40:1231–1234.

57. Albin RL, Young AB, Penney JB, et al. Abnormalities of striatal projection neurons and N-methyl-D-aspartate receptors in presymptomatic Huntington's disease. N Engl J Med 1990; 322:1293–1298.

58. Hansotia P, Cleeland CS, Chun RWM. Juvenile Huntington's chorea. Neurology 1968; 18:217–224.

59. Menkes JH. Textbook of child neurology. 4th ed. Philadelphia, Pa: Lea & Febiger, 1990.

60. Legido A, Zimmerman RA, Packer RJ, Bilaniuk LT, Siegel KR, D'Angio G. Significance of basal ganglia calcification on computed tomography in children. Pediatr Neurosci 1988; 14:64–70.

61. Kendall B, Cavanagh N. Intracranial calcification in paediatric computed tomography. Neuroradiology 1986; 28:324–330.

62. Harrington MG, Macpherson P, McIntosh WB, Allam BF, Bone I. The significance of the incidental finding of basal ganglia calcification on computed tomography. J Neurol Neurosurg Psychiatry 1981; 44:1168–1170.

63. Cohen CR, Duchesneau PM, Weinstein MA. Calcification of the basal ganglia as visualized by computed tomography. Radiology 1980; 134:97–99.

64. Henkelman RM, Watts JF, Kucharczyk W. High signal intensity in MR images of calcified brain tissue. Radiology 1991; 179:199–206.

65. McAdams HP, Geyer CA, Done SL, Deigh D, Mitchell M, Ghaed VN. CT and MR imaging in Canavan disease. AJNR 1990; 11:397–399.

66. Becker LE. Lysosomes, peroxisomes and mitochondria: function and disorder. AJNR 1992; 13:609–620.

67. Riccardi VM. Von Recklinghausen neurofibromatosis. N Engl J Med 1981; 305:1617–1627.

68. Boganno JR, Edwards MK, Lee TA, Dunn DW, Roos KL, Klatte EC. Cranial MR imaging in neurofibromatosis. AJNR 1988; 9:461–468.

69. Pont MS, Elster AD. Lesions of skin and brain: modern imaging of the neurocutaneous syndromes. AJR 1992; 158:1193–1203.

70. Aoki S, Barkovich AJ, Nishimura K, et al. Neurofibromatosis types 1 and 2: cranial MR findings. Radiology 1989; 172:527–534.

71. Sevick RJ, Barkovich AJ, Edwards MS, Koch TK, Lempert T, Norman D. Neurofibromatosis type 1: temporal evolution of white matter lesions (abstr). Radiology 1991; 181(P):193.

72. Mirowitz SA, Sartor K, Gado M. High-intensity basal ganglia lesions on T1-weighted MR images in neurofibromatosis. AJNR 1989; 10:1159–1163.